Hindawi
Complexity
Volume 2022, Article ID 2685573, 10 pages
https://doi.org/10.1155/2022/2685573

*Research Article*

# Suspension System Control Based on Type-2 Fuzzy Sliding Mode Technique

**Zheng Wang**,[1] **Longyi Ran**,[1] **Bing Kong**,[2] **Xuezeng Jia**,[1] **Liya Liu**,[1] **and Jafar Tavoosi**[3]

[1]*Chongqing Chemical Industry Vocational College, Chongqing 401220, China*
[2]*CNOOC China Limited, Tianjin Branch, Tianjin 300459, China*
[3]*Department of Electrical Engineering, Ilam University, Ilam, Iran*

Correspondence should be addressed to Zheng Wang; wz15923012499@sina.com and Jafar Tavoosi; j.tavoosi@ilam.ac.ir

Received 17 February 2022; Revised 21 April 2022; Accepted 27 April 2022; Published 24 May 2022

Academic Editor: Xiaoping Liu



This paper presents a new method of intelligent control for vehicle suspension. First, the suspension system is modeled with all the details, and then based on the obtained model, the sliding mode control is designed for it. The controller parameters and coefficients are calculated and updated by a type-2 fuzzy system. The chattering phenomenon is eliminated with a unique technique. In order to evaluate the performance of the proposed control system, two-model uncertainty of the road is applied. Simulations have been performed for both active and passive modes. The simulation results show the high efficiency of the proposed control system.

## 1. Introduction

A compromise between passenger convenience and the ability to direct vehicle is required in the design of the suspension system [1, 2]. To achieve the convenience of passengers, a soft suspension system is required to minimize the displacement and acceleration of the vehicle body. But, the suspension system must be stiff to direct vehicles in different road conditions [3, 4]. In a passive suspension system, spring and damper parameters are constant, so the vehicle body will fluctuate in the face of road terrain [4]. An active suspension system could adapt itself to different conditions of the road and decreases displacement and acceleration of the vehicle body simultaneously [5, 6]. A lot of research has been conducted to design the active suspensions system by different approaches (see [7] and its references).

One of the important advantages of sliding mode control (SMC) is invariance property to indeterminacy [8]. Considering this advantage, sliding mode control is a strong tool to confront parametric or nonparametric uncertainties, disturbances, and noise [9]. It is worth noting that invariance is a stronger property than robustness [10, 11]. Robustness means to achieve an optimal outcome in the worst conditions, and invariance means to achieve the optimal outcome without influencing the system with noise, disturbances, and indeterminacy. In the face of noise, disturbance, and uncertainty, a robust system may malfunction, while invariance means robustness with strong performance [12, 13]. Chattering is one of the bad properties of sliding phase; therefore, the arrival time to the sliding surface and arrival phase should be limited in a nonlinear system. Chattering is defined as high but limited frequencies fluctuates that cause heat loss in electrical equipment and depreciation of mechanical components [14]. Four methods have been proposed to decrease or eliminate chattering: boundary, adaptive boundary layer, higher-order sliding mode control (HOSMC), and dynamical SMC [15, 16]. Chattering was not eliminated but decreased in the boundary layer and adaptive boundary layer [17, 18]. In HOSMC, chattering is eliminated by transferring it to higher derivatives of the sliding surface [19, 20]. A lot of algorithms have been proposed to apply the second or higher order of sliding mode control [21]. Although model derivatives of the system are required for SMC calculations, for example, dynamical model derivatives of

the system are required for two relative degree systems [22]. While in dynamic sliding mode control, an integrator (or low-pass filter) is placed before the system, which causes to eliminate chattering because this filter eliminates high-frequency fluctuations [23]. The integrator increases the system degree; therefore, the model and dynamic of the system should be clear to apply sliding mode control on the additive system [24]. In other words, in dynamic sliding mode control, it is the required system model, but in HOSM, the model derivatives of the system should be clear. This case indicates precedence of dynamic on high degree.

In [25] fuzzy adaptive sliding mode, control has been used along with proportional-integral controller to apply in active suspension system. In the mentioned paper, the stability of the system is asymptotically proven and the convergence time of the system is long, so there is no sliding phase and chattering is not eliminated. Moreover, the sign function is emerged in the input signal directly, which makes chattering. Control methods such as PI and PID can also be used as appropriate solutions [26]. Applying nonlinear systems identification is also very important to have an accurate model of the system [27]. The proposed approach in [28] uses the proportional-integral sliding mode control for the quarter-car model, in which stability demonstration is asymptotical. Then, there is no sliding phase and so invariance is eliminated. In [29], Kalman filter applies on nonlinear model of Quarter-Car suspension system to estimate linear model states. Moreover, due to stability proof being asymptotical, the sliding phase does not exist, and chattering is eliminated. In [30], linearization of hydraulic actuator equation is used firstly. Then, a dynamic sliding mode controller is applied in the output control loop. The authors have not considered the servo valve equation to simplify applying feedback linearization, and the closed-loop system has no invariance property because feedback linearization is not robust. Fewer people today do not own a vehicle or use a car, so an active and intelligent suspension is essential for the well-being of the car occupants. This article deals with this issue in detail and the ultimate goal is to design an active suspension system with minimal oscillation and vibration.

In this paper, for the first time, we use a recurrent type-2 fuzzy to update SMC coefficients for use in the suspension system. Another innovation of this article is the use of SMC with three terms (while others have used two-term SMC). As can be seen in (12), there are three $\lambda$, but in the other's work, there are two $\lambda$, meaning that they set only two parameters. So, our SMC also has greater degree of freedom that can control the system more precisely. Also, in this paper, road roughness is applied by two models in transparent manners and it is observed that the active suspension system with fuzzy neural network has a better response.

The main contribution of this paper is as follows:

(1) Propose a new recurrent type-2 fuzzy system to update the SMC coefficients for use in the suspension system. Figure 1 (page 6) shows a new structure of the type-2 fuzzy neural network, which is carefully observed in (13) that weights are also type-2 fuzzy sets (in addition to membership functions.)

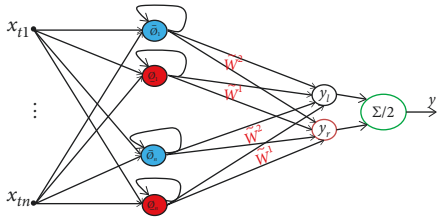


Figure 1: The structure of the proposed type-2 fuzzy system.

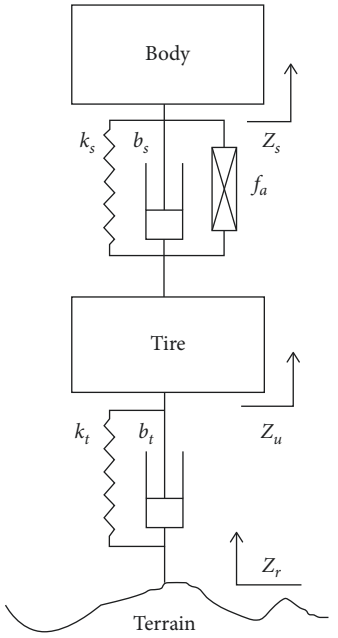


Figure 2: Quarter-car suspension system.

(2) Another innovation of this article is the use of SMC with three terms (while others have used two-term SMC). As can be seen in (15), there are three $\lambda$, but in the other's work, there are two $\lambda$, meaning that they set only two parameters. So, our SMC also has greater degree of freedom that can control the system more precisely.

(3) Also, in this paper, road roughness is applied by two models in transparent manners (in similar articles, only one type of roughness has been investigated) and it is observed that the active suspension system with fuzzy neural network has a better response.

In Section 2, dynamic components of the applied suspension system are explained. In Section 3, the proposed approach and question definition are presented. The controller design is presented in Section 4. Important notes in the proposed approach are stated in Section 5. Simulation and conclusion are considered in Sections 6 and 7, respectively.

## 2. Dynamic Model of the Suspension System

The dynamics of the intended active suspension system of a quarter-car, which is described by the following equations, is shown in Figure 2

$$m_s\ddot{z}_s = -b_s(\dot{z}_s - \dot{z}_u) - k_s(z_s - z_u) + f_a, \tag{1}$$

$$\begin{aligned} m_u\ddot{z}_u &= +b_s(\dot{z}_s - \dot{z}_u) + k_s(z_s - z_u) - f_a \\ &\quad + b_t(\dot{z}_r - \dot{z}_u) + k_t(z_r - z_u), \end{aligned} \tag{2}$$

where $z_s$, $z_u$, and $z_r$ are the vertical displacement of the body and wheels and height of land terrains to baseline, respectively. Also, the first and second derivatives $z_s$ and $z_u$ indicate the vertical velocity and acceleration of vehicle body and wheels. Note that we assume velocity and acceleration in the system are perpendicular to the ground. In addition, $m_s$, $m_u$, $k_s$, $k_t$, $b_s$, and $b_t$ are the mass, stiffness, vehicle body, damping, and wheels, $z_s - z_u$ is the suspension deflection, and $z_u - z_r$ is the wheel deflection. Variable $f_a$ $e$ is the output force of the hydraulic actuator, which is placed between the body and wheels. If $f_a = 0$, the intended suspension system will be inactive.

To design an active suspension system, the desired $f_a$ value should be determined so that $z_s$, $\dot{z}_s$, and $\ddot{z}_s$ have the minimum value. We assume that all parameters are defined, and all variables are measurable. This assumption is logical because the variables can measure with different sensors in a mechanical system. In practical applications, sensors are installed on the vehicle and are used then. $z_r$ and its derivative are the only variables that are not measurable practically that is considered as indeterminacy. This structure is shown in Figure 2. The servo valve equations activate the hydraulic actuator as follows. It is worth noting that the input of the valve is current too.

$$\dot{x}_{\mathrm{sp}} = \frac{\left(-x_{\mathrm{sp}} + i_{\mathrm{sv}}\right)}{\tau}, \tag{3}$$

where $i_{\mathrm{sv}}$ is the input current of the valve and $\tau$ is the mechanical time constant of the servo valve, and $x_{\mathrm{sp}}$ is the spool valve displacement (or input) which is attached to the hydraulic actuator. Dynamic equations of the hydraulic actuator are as follows:

$$\dot{f}_a = -\alpha A_p^2(\dot{z}_s - \dot{z}_u) - \beta f_a + \gamma A_p x_{\mathrm{sp}} \sqrt{P_s - \frac{B_{\mathrm{kl}}\left(x_{\mathrm{sp}}\right) f_a}{A_p}}, \tag{4}$$

where $B_{\mathrm{kl}}$ represents the backlash in the output of the solenoid valve depicted in Figure 3. For this figure, we have $a = b = 0.1$. It should be noted that the derivative of the output with respect to the input is always either 0 or 1.

As seen in (3) and (4), $i_{\mathrm{sv}}$ is the only input and the only parameter required to be calculated to reach the optimal $f_a$. This structure as well is demonstrated in Figure 4 where $P_s$ and $P_r$ are the direct and return pressures of the actuator, respectively, and $P_u$ and $P_l$ are the pressures in the upper and lower of the actuator cylinder chambers, respectively. Plus, $A_p$ is the piston area and $\beta = \alpha C_{\mathrm{tp}}, \cdot \alpha = 4\beta_e/V_t, \cdot \gamma = \alpha C_d w\sqrt{1/\rho}$ where $\beta_e$ is the bulk modulus of hydraulic fluid, $V_t$ is the volume of the hydraulic cylinder, $C_{tp}$ is the leakage coefficient, $C_d$ is the discharge coefficient, $w$ is the spool valve area gradient, and $\rho$ is the hydraulic oil density.

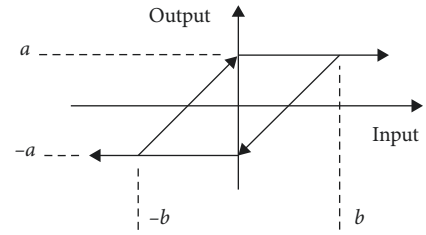


Figure 3: Backlash of hydraulic actuator.

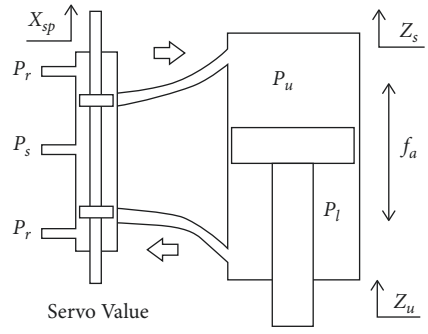


Figure 4: Hydraulic actuator system with double active.

## 3. Problem Description

The recommended method has two steps. In the first step, we assume $f_a$ is the input of system (1). In this case, by controlling the dynamic sliding mode, the desired smooth and free of chattering, that is, $f_d$ will be calculated such that the dislocation, velocity, and acceleration of the car body ($z_s$, $\dot{z}_s$, and $\ddot{z}_s$, respectively) converge to 0, leading to more comfort of the passengers.

In the second step, using another dynamic sliding mode control, the smooth and free of chattering current of the solenoid valve $i_{\mathrm{sv}}$ will be determined such that in (4), $f_a$ follows the optimal $f_d$ value obtained in the first step.

To apply the suggested method, we define the following state variables of (1):

$$\begin{aligned} x_1 &= z_S, \\ x_2 &= \dot{z}_S, \end{aligned} \tag{5}$$

Hence,

$$\begin{aligned} \dot{x}_1 &= x_2, \\ \dot{x}_2 &= -\frac{b_s}{m_s}x_2 - \frac{k_s}{m_s}x_1 + \frac{b_s}{m_s}\dot{z}_u + \frac{k_s}{m_s}z_u + \frac{f_a}{m_s}. \end{aligned} \tag{6}$$

On the other hand, (2) can be rewritten as

$$\begin{aligned} \ddot{z}_u &= \frac{b_s}{m_u}x_2 + \frac{k_s}{m_u}x_1 + \left(-\frac{b_s}{m_u} - \frac{b_t}{m_u}\right)\dot{z}_u \\ &\quad + \left(-\frac{k_s}{m_u} - \frac{k_t}{m_u}\right)z_u - \frac{f_a}{m_u} + f_{\mathrm{dis}}. \end{aligned} \tag{7}$$

Also, as stated, $f_{\mathrm{dis}}$ that represents the terrains on the ground is considered as the uncertainty,

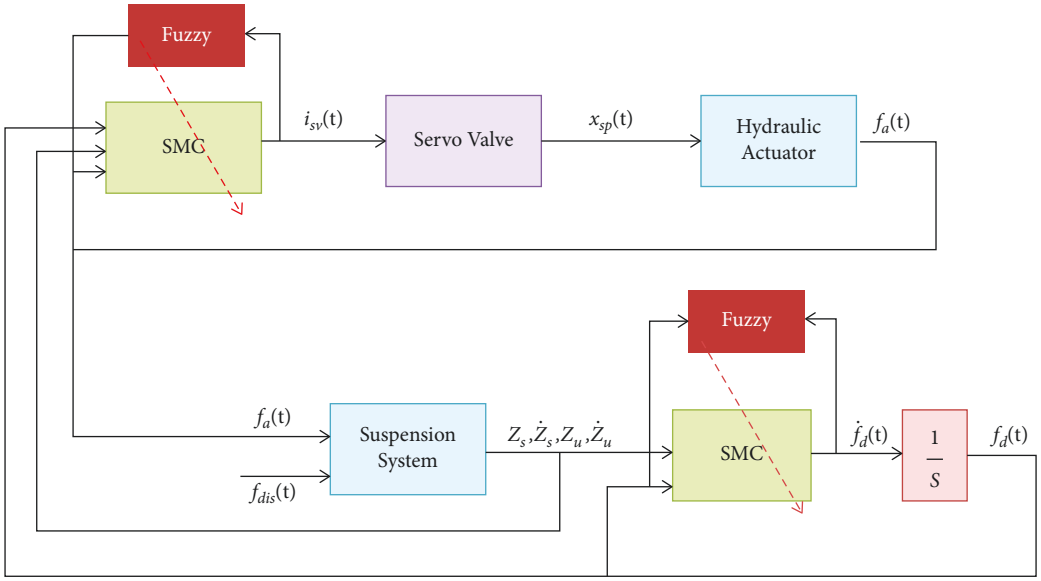


Figure 5: Block diagram of the proposed control system.

$$f_{\text{dis}} = \frac{b_t}{m_u}\dot{z}_r + \frac{k_t}{m_u}z_r. \tag{8}$$

Also, (4) can be reformulated as well.

$$\dot{f}_a = -\beta f_a - \alpha A_p^2 x_2 + \alpha A_p^2 \dot{z}_u + \gamma A_p x_{\text{sp}} g\left(x_{\text{sp}}, f_a\right), \tag{9}$$

where

$$g = \sqrt{P_s - \frac{B_{\text{kl}}\left(x_{\text{sp}}\right) f_a}{A_p}}. \tag{10}$$

## 4. Type-2 Fuzzy System

In this section, the proposed type-2 fuzzy system is discussed to predict the parameters of SMC. Numerous studies have shown that type-2 fuzzy system performs better than type-1 fuzzy system. Figure 3 shows the structure of the proposed type-2 fuzzy system.

$$\left\{ \overline{\varnothing}_{ji}\left(u_j\right) = \begin{cases} \left(u_j - c_{ji}^1\right)^2, & u_j < c_{ji}^1, \\ 1, & c_{ji}^1 \le u_j \le c_{ji}^2, \\ \left(u_j - c_{ji}^2\right)^2 & u_j > c_{ji}^2, \end{cases} \varnothing_{ji}\left(u_j\right) = \begin{cases} \left(u_j - c_{ji}^2\right)^2, & u_j \le \dfrac{c_{ji}^1 + c_{ji}^2}{2}, \\ \left(u_j - c_{ji}^1\right)^2 & u_j > \dfrac{c_{ji}^1 + c_{ji}^2}{2}, \end{cases} \right. \tag{11}$$

where $\overline{\varnothing}_{ji}$ and $\varnothing_{ji}$ are the upper and lower of the $j^{\text{th}}$ input and $i^{\text{th}}$ neuron, respectively. Therefore, the outputs of the first layer are as follows:

The type-2 fuzzy neural network presented is completely new (both membership functions and weights are type-2 fuzzy sets) and is used for the first time in this article. This type-2 fuzzy neural network is used to update sliding mode control parameters (equation (15), $\lambda\_1$, $\lambda\_2$, $\lambda\_3$) according to the amount of error. Figure 5 shows that the fuzzy system considers the system parameters online and tunes the $\lambda$ parameters. In the work of others, these parameters are determined in trial and error way, but in our work, the parameters are calculated online based on changes in system's dynamic. In the proposed method, data are first collected to train the neural network. At this stage, rich data are extracted both for the error-free system and by applying some deliberate errors to the system. Naturally, the more the system dynamics can be changed and the more the errors applied, the more useful the data will be obtained for neural network training.

The internal phase of the first layer calculations is given as follows:

$$\left\{ \overline{\varnothing}_i(u) = \exp\left(-\frac{\sum_{j=1}^{n+1} \overline{\varnothing}_{ji}\left(u_j\right)}{\sigma_i^2}\right), \varnothing_i(u) = \exp\left(-\frac{\sum_{j=1}^{n+1} \varnothing_{ji}\left(u_j\right)}{\sigma_i^2}\right), \right. \tag{12}$$

where $\overline{\varnothing}_i$ and $\varnothing_i$ are the upper and lower of the $i^{\text{th}}$ neuron ($i = 1, 2, \ldots, m$), respectively. $u \in (u_j)$, $j = 1, \ldots, n$ is the input vector, and $c_{\text{ji}} \in [c_{\text{ji}}^1, c_{\text{ji}}^2]$ is the center of all the RBF

neurons. It should be noted that the left and right endpoints of the second layer are as follows:

$$\begin{cases} \hat{y}_l = \dfrac{\sum_{i=1}^{q} \overline{\varnothing}_i(u) c_{w_i}^2 \sigma_{w_i} + \sum_{i=q+1}^{m} \varnothing_i(u) c_{w_i}^1 \sigma_{w_i}}{\sum_{i=1}^{q} \overline{\varnothing}_i(u) \sigma_{w_i} + \sum_{i=q+1}^{m} \varnothing_i(u) \sigma_{w_i}} \\ \hat{y}_r = \dfrac{\sum_{i=1}^{p} \varnothing_i(u) c_{w_i}^1 \sigma_{w_i} + \sum_{i=p+1}^{m} \overline{\varnothing}_i(u) c_{w_i}^2 \sigma_{w_i}}{\sum_{i=1}^{p} \varnothing_i(u) \sigma_{w_i} + \sum_{i=p+1}^{m} \overline{\varnothing}_i(u) \sigma_{w_i}}, \end{cases} \tag{13}$$

where $p$ and $q$ are the left and right switching points of the type-2 fuzzy system, which can be calculated using the trial and error method or the Karnik–Mendel (KM) algorithm. Also, $m$, $w_i$, $c_{w_i}$, and $\sigma_{w_i}$ are the mean values of the first layer neurons, the weights, the center of weights, and the spread of weights, respectively. Lastly, the general output of the network can be derived as follows:

$$\hat{y} = \frac{\hat{y}_l + \hat{y}_r}{2}. \tag{14}$$

The gradient descent method is used to teach the network. See [31, 32], for more details.

## 5. The Designing of the Active Controller

As stated, $f_a$ is considered as the dynamic input control signal (6) and is determined such that $z_s$, $\dot{z}_s$, and $\ddot{z}_s$ ($x_1$, $x_2$, $x_3 = \dot{x}_2$) converge to 0 in a limited time. The calculated value is the desirable force that needs to be generated by the hydraulic actuator. We name it $f_d$ and determine it using the dynamic sliding mode control. To execute this controller, the sliding surface $s$ is defined as

$$s = \lambda_1 x_1 + \lambda_2 x_2 + \lambda_3 x_3. \tag{15}$$

The optimal values of the control parameters $(\lambda_1, \lambda_2, \lambda_3)$ are calculated at any time by the type-2 fuzzy system. We determine the constant coefficients of the surface so that the following equation is Hurwitz:

$$\lambda_3 p^2 + \lambda_2 p + \lambda_1 = 0. \tag{16}$$

The derivative of this surface is

$$\dot{s} = \lambda_1 \dot{x}_1 + \lambda_2 \dot{x}_2 + \lambda_3 \dot{x}_3 = \lambda_1 x_2 + \lambda_2 x_3 + \lambda_3 \dot{x}_3. \tag{17}$$

Now, using (6), we have

$$\dot{x}_3 = \ddot{x}_2 = -\frac{b_s}{m_s} x_3 - \frac{k_s}{m_s} x_2 + \frac{b_s}{m_s} \ddot{z}_u + \frac{k_s}{m_s} \dot{z}_u + \frac{\dot{f}_d}{m_s}. \tag{18}$$

Using this equation, the derivative of the sliding surface is

$$\begin{aligned} \dot{s} = {} & \lambda_1 (x_2) \\ & + \lambda_2 \left( -\frac{b_s}{m_s} x_2 - \frac{k_s}{m_s} x_1 + \frac{b_s}{m_s} \dot{z}_u + \frac{k_s}{m_s} z_u + \frac{f_d}{m_s} \right) \\ & + \lambda_3 \left( -\frac{b_s}{m_s} x_3 - \frac{k_s}{m_s} x_2 + \frac{b_s}{m_s} \ddot{z}_u + \frac{k_s}{m_s} \dot{z}_u + \frac{\dot{f}_d}{m_s} \right). \end{aligned} \tag{19}$$

This equation can be reformulated as

$$\begin{aligned} \dot{s} = {} & \left( \lambda_1 - \frac{\lambda_2 b_s}{m_s} - \frac{\lambda_3 k_s}{m_s} \right) x_2 + \left( -\frac{\lambda_2 k_s}{m_s} \right) x_1 \\ & + \left( \frac{\lambda_2 b_s}{m_s} + \frac{\lambda_3 k_s}{m_s} \right) \dot{z}_u + \left( \frac{\lambda_2 k_s}{m_s} \right) z_u \\ & + \left( \frac{\lambda_2 f_d}{m_s} + \frac{\lambda_3 \dot{f}_d}{m_s} \right) + \left( -\frac{\lambda_3 b_s}{m_s} \right) x_3 + \left( \frac{\lambda_3 b_s}{m_s} \right) \ddot{z}_u. \end{aligned} \tag{20}$$

Now, we replace the $\ddot{z}_u$ from (7) into (16)

$$\begin{aligned} \dot{s}| = {} & \left( \lambda_1 - \frac{\lambda_2 b_s}{m_s} - \frac{\lambda_3 k_s}{m_s} + \frac{\lambda_3 b_s}{m_s} \frac{b_s}{m_u} \right) x_2 \\ & + \left( -\frac{\lambda_2 k_s}{m_s} + \frac{\lambda_3 b_s}{m_s} \frac{k_s}{m_u} \right) x_1 \\ & + \left( \frac{\lambda_2 b_s}{m_s} + \frac{\lambda_3 k_s}{m_s} - \frac{\lambda_3 b_s}{m_s} \frac{b_s}{m_u} - \frac{\lambda_3 b_s}{m_s} \frac{b_t}{m_u} \right) \dot{z}_u \\ & + \left( \frac{\lambda_2 k_s}{m_s} + \frac{\lambda_3 b_s}{m_s} \frac{k_s}{m_u} - \frac{\lambda_3 b_s}{m_s} \frac{k_t}{m_u} \right) z_u + \left( \frac{\lambda_3}{m_s} \right) \dot{f}_d \\ & + \left( \frac{\lambda_2}{m_s} - \frac{\lambda_3 b_s}{m_s} \frac{1}{m_u} \right) f_d + \left( -\frac{\lambda_3 b_s}{m_s} \right) + \left( \frac{\lambda_3 b_s}{m_s} \right) f_{dis}. \end{aligned} \tag{21}$$

Again, considering that $x_3 = \dot{x}_2$, we have

$$\begin{aligned} \dot{s}| = {} & \left( \lambda_1 - \frac{\lambda_2 b_s}{m_s} - \frac{\lambda_3 k_s}{m_s} + \frac{\lambda_3 b_s}{m_s} \frac{b_s}{m_u} + \frac{\lambda_3 b_s}{m_s} \frac{b_s}{m_u} \right) x_2 \\ & + \left( -\frac{\lambda_2 k_s}{m_s} + \frac{\lambda_3 b_s}{m_s} \frac{k_s}{m_u} + \frac{\lambda_3 b_s}{m_s} \frac{k_s}{m_u} \right) x_1 + \left( \frac{\lambda_3}{m_s} \right) \dot{f}_d \\ & + \left( \frac{\lambda_2}{m_s} + \frac{\lambda_3 b_s}{m_s} \frac{1}{m_u} - \frac{\lambda_3 b_s}{m_s} \frac{1}{m_u} \right) f_d + \left( \frac{\lambda_3 b_s}{m_s} \right) f_{dis} \\ & + \left( \frac{\lambda_2 b_s}{m_s} + \frac{\lambda_3 k_s}{m_s} - \frac{\lambda_3 b_s}{m_s} \frac{b_s}{m_u} - \frac{\lambda_3 b_s}{m_s} \frac{b_t}{m_u} - \frac{\lambda_3 b_s}{m_s} \frac{b_s}{m_s} \right) \dot{z}_u \\ & + \left( \frac{\lambda_3 b_s}{m_s} + \frac{\lambda_3 b_s}{m_s} \frac{k_s}{m_u} - \frac{\lambda_3 b_s}{m_s} \frac{k_t}{m_u} - \frac{\lambda_3 b_s}{m_s} \frac{k_s}{m_u} \right) z_u. \end{aligned} \tag{22}$$

For the purpose of simplicity, (22) can be rewritten using the corresponding coefficients:

$$\begin{aligned} \dot{s} = {} & k_1 x_1 + k_2 x_2 + k_3 z_u + k_4 \dot{z}_u \\ & + k_5 f_d + k_6 \dot{f}_d + k_7 f_{\text{dis}}. \end{aligned} \tag{23}$$

**Theorem 1.** *The following desirable input for the system (1) or (6) converges the states $x_1$, $x_2$, $x_3$ to 0 in a limited time.*

$$\dot{f}_d = -\frac{k_1x_1 + k_2x_2 + k_3z_u + k_4\dot{z}_u + k_5f_d + \eta f_s}{k_6}, \quad \eta = |k_7 f_{\text{dis}}| + \varepsilon, \varepsilon > 0, \tag{24}$$

*where $f_s = sat(s/\varphi)$ is the saturation function and $\phi$ is the thickness of the border layer.*

*Proof.* Considering the $V = 0.5s^2$ Lyapunov function, we have

$$\begin{aligned}\dot{V} = s\dot{s} &= s\left(k_1x_1 + k_2x_2 + k_3z_u + k_4\dot{z}_u + k_5f_d\right.\\ &\left.+k_6\dot{f}_d + k_7f_{\text{dis}}\right) = s\left(k_7f_{\text{dis}} - \eta f_s\right) = \text{sk}_7f_{\text{dis}} - \eta|f_s|\\ &\le |k_7f_{\text{dis}}\|s| - \eta|f_s| = \left(|k_7f_{\text{dis}}| - \eta\right)|s| = -\varepsilon|s| \le 0.\end{aligned} \tag{25}$$

This concludes $t_s \le |s(0)|/\varepsilon$ where $t_s$ ,the limited time of the states, is reaching the marginal layer around the sliding surface. The suggested controller is pictured in Figure 1. □

*5.1. Calculation of the Valve Current (Step 2).* The purpose of this step is the calculation of $i_{\text{sv}}$ from (3) such that $f_a$ in (4) or (9) follows the $f_d$ desirable value that is obtainable in the first step from equation (24). To this end and to obtain a smooth and free of chattering $i_{sv}$ that is practical, the dynamic sliding mode control is employed. Now, the sliding surface is defined:

$$s_f = \lambda_4\left(\dot{f}_a - \dot{f}_d\right) + \lambda_5\left(f_a - f_d\right). \tag{26}$$

Note that the optimal values of the control parameters $(\lambda_4, \lambda_5)$ are calculated at any time by the type-2 fuzzy system. Also, the constant coefficients will be determined so that the following equation is Hurwitz:

$$\lambda_4 p + \lambda_5 = 0. \tag{27}$$

The derivative of this surface is

$$\dot{s}_f = \lambda_4\left(\ddot{f}_a - \ddot{f}_d\right) + \lambda_5\left(\dot{f}_a - \dot{f}_d\right). \tag{28}$$

By replacing $\ddot{f}_a$ from (4) and $\ddot{f}_d$ from (20), we have

$$\begin{aligned}\dot{s}_f &= \lambda_4\left(\ddot{f}_a - \ddot{f}_d\right) + \lambda_5\left(\dot{f}_a - \dot{f}_d\right)\\ &= \lambda_4\left(-\beta\dot{f}_a - \alpha A_p^2\dot{x}_2 + \alpha A_p^2\ddot{z}_u + \gamma A_p\dot{x}_{\text{sp}}g + \gamma A_px_{\text{sp}}\dot{g}\right)\\ &\quad + \lambda_4\left(\frac{k_1x_2 + k_2\dot{x}_2 + k_3\dot{z}_u + k_4\ddot{z}_u + k_5\dot{f}_d + \eta\dot{f}_s}{k_6}\right)\\ &\quad + \lambda_5\left(-\beta f_a - \alpha A_p^2x_2 + \alpha A_p^2\dot{z}_u + \gamma A_px_{\text{sp}}g\right)\\ &\quad + \lambda_5\left(\frac{k_1x_1 + k_2x_2 + k_3z_u + k_4\dot{z}_u + k_5f_d + \eta f_s}{k_6}\right).\end{aligned} \tag{29}$$

This can be organized as

$$\begin{aligned}\dot{s}_f &= \left(-\lambda_4\alpha A_p^2 + \lambda_4\frac{k_2}{k_6}\right)\dot{x}_2\\ &\quad + \left(-\lambda_5\alpha A_p^2 + \lambda_4\frac{k_1}{k_6} + \lambda_5\frac{k_2}{k_6}\right)x_2 + \left(\lambda_5\frac{k_1}{k_6}\right)x_1\\ &\quad + \left(\lambda_4\alpha A_p^2 + \lambda_4\frac{k_4}{k_6}\right)\ddot{z}_u + \left(\lambda_4\frac{\eta}{k_6}\right)\dot{f}_s\\ &\quad + \left(\lambda_5\alpha A_p^2 + \lambda_5\frac{k_4}{k_6} + \lambda_4\frac{k_3}{k_6}\right)\dot{z}_u + \left(\lambda_5\frac{k_3}{k_6}\right)z_u\\ &\quad + \left(-\lambda_4\beta\right)\dot{f}_a + \left(-\lambda_5\beta\right)f_a + \left(\lambda_4\gamma A_pg\right)\dot{x}_{\text{sp}}\\ &\quad + \left(\lambda_4\gamma A_p\dot{g} + \lambda_5\gamma A_pg\right)x_{\text{sp}} + \left(\lambda_4\frac{k_5}{k_6}\right)\dot{f}_d\\ &\quad + \left(\lambda_5\frac{k_5}{k_6}\right)f_d + \left(\lambda_5\frac{\eta}{k_6}\right)f_s.\end{aligned} \tag{30}$$

By replacing $\dot{x}_2$, $\ddot{z}_u$, $\dot{f}_a$, $\dot{f}_d$, and $\dot{x}_{sp}$, we have

$$\begin{aligned}\dot{s}_f = &+\left\{\begin{array}{l}-\frac{k_2}{k_6}\lambda_4\frac{k_5}{k_6} - \alpha A_p^2\left(-\lambda_4\beta\right) + \frac{b_s}{m_u}\left(\lambda_4\alpha A_p^2 + \lambda_4\frac{k_4}{k_6}\right)\\ -\frac{b_s}{m_u}\left(-\lambda_4\alpha A_p^2 + \lambda_4\frac{k_2}{k_6}\right) - \lambda_5\alpha A_p^2 + \lambda_4\frac{k_1}{k_6} + \lambda_5\frac{k_{21}}{k_6}\end{array}\right\}x_2\\ &+\left\{\begin{array}{l}-\frac{k_1}{k_6}\lambda_4\frac{k_5}{k_6} + \frac{k_s}{m_u}\left(\lambda_4\alpha A_p^2 + \lambda_4\frac{k_4}{k_6}\right)\\ -\frac{k_s}{m_u}\left(-\lambda_4\alpha A_p^2 + \lambda_4\frac{k_2}{k_6}\right) + \lambda_5\frac{k_1}{k_6}\end{array}\right\}x_1\\ &+\left\{\begin{array}{l}-\frac{k_4}{k_6}\lambda_4\frac{k_5}{k_6} + \alpha A_p^2\left(-\lambda_4\beta\right)\lambda_4\frac{k_3}{k_6}\\ -\left(\frac{b_s}{m_u} - \frac{b_t}{m_u}\right)\left(\lambda_4\alpha A_p^2 + \lambda_4\frac{k_4}{k_6}\right)\\ +\frac{b_s}{m_s}\left(-\lambda_4\alpha A_p^2 + \lambda_4\frac{k_2}{k_6}\right) + \lambda_5\alpha A_p^2 + \lambda_5\frac{k_4}{k_6}\end{array}\right\}\dot{z}_u\\ &+\left\{\begin{array}{l}-\frac{k_3}{k_6}\lambda_4\frac{k_5}{k_6} + \left(-\frac{k_s}{m_u} - \frac{k_t}{m_u}\right)\left(\lambda_4\alpha A_p^2 + \lambda_4\frac{k_4}{k_6}\right)\\ -\frac{k_s}{m_s}\left(-\lambda_4\alpha A_p^2 + \lambda_4\frac{k_2}{k_6}\right) + \lambda_5\frac{k_3}{k_6}\end{array}\right\}z_u\\ &+\left\{\begin{array}{l}-\beta\left(-\lambda_4\beta\right) - \frac{1}{m_u}\left(\lambda_4\alpha A_p^2 + \lambda_4\frac{k_4}{k_6}\right)\\ +\frac{1}{m_s}\left(-\lambda_4\alpha A_p^2 + \lambda_4\frac{k_2}{k_6}\right) + \lambda_5\beta\end{array}\right\}f_a\\ &+\left\{-\frac{1}{\tau}\left(\lambda_4\gamma A_pg\right) + \gamma A_pg\left(-\lambda_4\beta\right) + \frac{1}{\tau}\left(\lambda_4\gamma A_pg\right)\right\}i_{sv}\\ &+\left\{+\lambda_4\gamma A_p\dot{g} + \lambda_5\gamma A_pg\right\}x_{\text{sp}}\\ &+\left\{-\frac{k_5}{k_6}\lambda_4\frac{k_5}{k_6} + \lambda_5\frac{k_5}{k_6}\right\}f_d + \left\{-\frac{\eta}{k_6}\lambda_4\frac{k_5}{k_6} + \lambda_5\frac{\eta}{k_6}\right\}f_s\\ &+\left\{\lambda_4\frac{\eta}{k_6}\right\}\dot{f}_s + \left\{\lambda_4\alpha A_p^2 + \lambda_4\frac{k_4}{k_6}\right\}f_{\text{dis}}.\end{aligned} \tag{31}$$

This can be simplified as

$$\dot{s}_f = k_8 x_1 + k_9 x_2 + k_{10} z_u + k_{11} \dot{z}_u + k_{12} f_a + k_{13} f_d + k_{14} x_{\text{sp}} + k_{15} i_{\text{sv}} + k_{16} f_s + k_{17} \dot{f}_s + k_{18} f_{\text{dis}}. \tag{32}$$

**Theorem 28.** *The following input for systems (3) and (4) or (3) and (9) causes $f_a - f_d$ to converge to 0 in a limited time.*

$$i_{\text{sv}} = -\frac{\eta_2 f_{\text{sf}} + k_{16} f_s + k_{17} \dot{f}_s + k_8 x_1 + k_9 x_2}{k_{15}} - \frac{k_{10} z_u + k_{11} \dot{z}_u + k_{12} f_a + k_{13} f_d + k_{14} x_{\text{sp}}}{k_{15}}, \tag{33}$$

$$\eta_2 = \left| k_{18} f_{\text{dis}} \right| + \varepsilon, \varepsilon > 0,$$

*where $f_{sf} = sat(s_f/\varphi)$ is the saturation function and $\phi$ is the thickness of the marginal layer.*

*Proof.* Considering the Lyapunov function $V = 0.5 s_f^2$, we have

$$\begin{aligned} \dot{V} &= s_f \dot{S}_f = s_f \left( k_8 x_1 + k_9 x_2 + k_{10} z_u + k_{11} \dot{z}_u + k_{12} f_a \right. \\ &\quad \left. + k_{13} f_d + k_{14} x_{\text{sp}} + k_{15} i_{\text{sv}} + k_{16} f_s + k_{17} \dot{f}_s + k_{18} f_{\text{dis}} \right) \\ &= s_f \left( k_{18} f_{\text{dis}} - \eta_2 f_{\text{sf}} \right) = s_f k_{18} f_{\text{dis}} - \eta_2 \left| f_{\text{sf}} \right| \\ &\le \left| k_{18} f_{\text{dis}} \right| \left| s_f \right| - \eta_2 \left| f_{\text{sf}} \right| = \left( \left| k_{18} f_{\text{dis}} \right| - \eta_2 \right) \left| s_f \right| \\ &= -\varepsilon \left| s_f \right| \le 0. \end{aligned} \tag{34}$$

This concludes $t_s \le |s(0)|/\varepsilon$ where $t_s$ is the limited time of the states reaching the marginal layer around the sliding surface. The general structure of the proposed controller is shown in Figure 5. As can be seen in this structure, using the dynamic sliding mode control of the current without chattering of the solenoid, inlet $i_{sv}$ is determined so that the output force of the hydraulic actuator follows our desired force. In other words, it is defined such that $f_a - f_d$ converges to zero in a limited time. On the other hand, this optimum force is determined and calculated by controlling the dynamic sliding state and mechanical equations of the suspension system to have the desired conditions of the passenger and the vehicle. Note that in (24), there is a sign function or discontinuity in $\dot{f}_d$ and is therefore without switching, because the integrator acts as a low-pass filter. The same is true for $i_{\text{sv}}$ and $x_{\text{sp}}$ in (3) and (33), and as a result, they are smooth and without chattering.

According to the second part of (6), the dynamic slip mode control causes $x_1$, $x_2$, $an\ d\ x_3 = \dot{x}_2$ to converge to zero and as a result,

$$b_s \dot{z}_u + k_s z_u = -f_d, \tag{35}$$

meaning that signals $z_u$ and $\dot{z}_u$ are also under control indirectly.

In case of using the ordinary (instead of the dynamic) sliding mode control to obtain $i_{\text{sv}}$ in (33), $x_{\text{sp}}$ is calculated instead of $i_{\text{sv}}$. This yields the emergence of a discontinuity in $x_{\text{sp}}$. Plus, the differential (3) needs to be solved. The solution of (3) means using an integrator that will increase the noise effect plus pay attention, that in the ordinary sliding mode control, the surface is defined as

$$s_f = \lambda_5 (f_a - f_d). \tag{36}$$

In this case, a chattering will appear in $f_a$ during the calculation. □

Table 1: Parameters of suspension system.

| Unit (dimension) | Value | Variable |
|---|---|---|
| Kg | 240 | $m_s$ |
| N/(m/s) | 375 | $b_s$ |
| N/m | 14600 | $k_s$ |
| Kg | 45 | $m_u$ |
| N/(m/s) | 415 | $b_t$ |
| N/m | 124600 | $k_t$ |
| $s^{-1}$ | 1 | $\beta$ |
| $m^2$ | $3.3 \times 10^{-4}$ | $A_p$ |
| S | 1.30 | $\tau$ |
| $N/m^5$ | $4.51 \times 10^{13}$ | $\alpha$ |
| Pa | 10342500 | $P_s$ |
| $N/m^{5/2}\text{kg}^{1/2}$ | $1.54 \times 10^9$ | $\gamma$ |

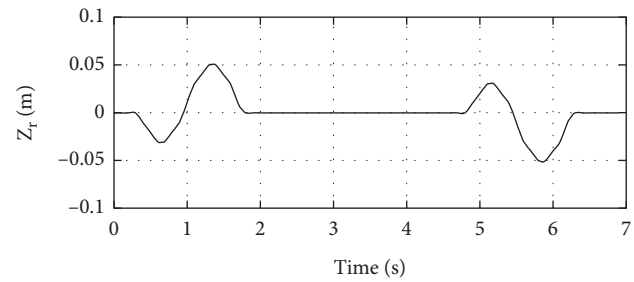


Figure 6: Terrain of the road 1.

## 6. Simulation

In this article, MATLAB software version 2019a has been used to model the suspension system and implement the proposed control system. The values of the parameters used for the suspension system are listed in Table 1 [7]. Plus, the initial values of the controller parameters are chosen as

$$\lambda_1 = 1, \lambda_2 = 6, \lambda_3 = 6, \lambda_4 = 10, \lambda_5 = 0.2, \varepsilon = 20, \varphi = 0.3. \tag{37}$$

To simulate, the terrains of the ground as the uncertainty are applied to the wheels as

$$z_r = \begin{cases} -0.05 \sin(t), & 0.3 \le t \le 1.8, \\ 0.05 \sin(t), & 4.8 \le t \le 6.3, \\ 0, & \text{otherwise.} \end{cases} \tag{38}$$

The simulation was performed with the MATLAB software with sample time of 0.01 for a period of 7 seconds in the active and inactive doses, and the results are shown in Figures 6 to 15. In the simulations, two types of roughness

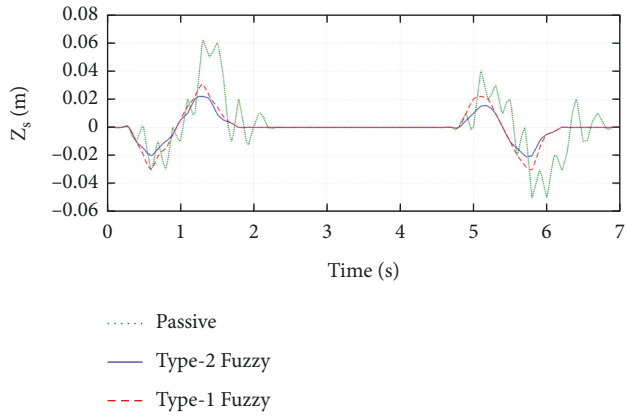


Figure 7: Body displacement.

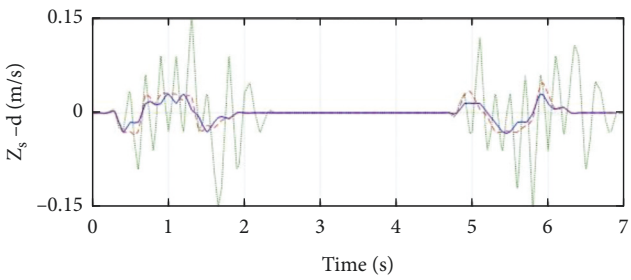


Figure 8: Body velocity.

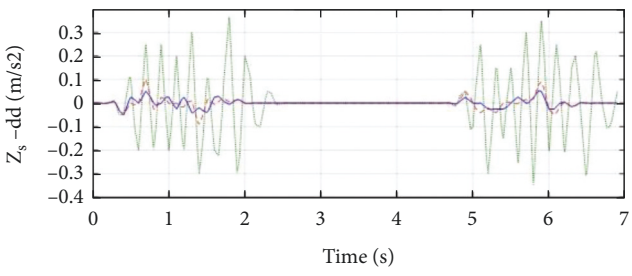


Figure 9: Body acceleration.

have been applied on the road. The first case is shown in Figure 6.

Figure 7 shows the results of the car body displacement control signal for both passive and active controller (sliding mode control with type-1 fuzzy and type-2 fuzzy systems).

Figure 8 shows the results of the vehicle body speed with all three control systems.

The acceleration of the vehicle body is very important in the comfort of the occupants and also in maintaining

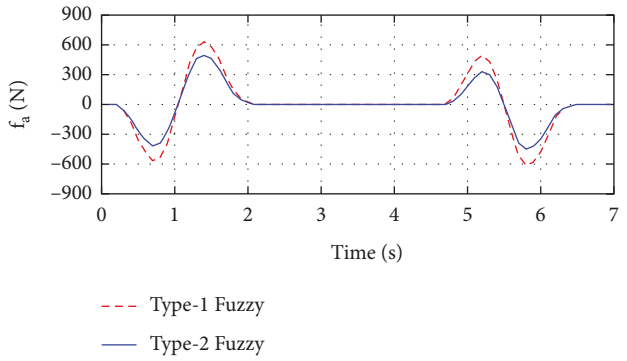


Figure 10: Control signal.

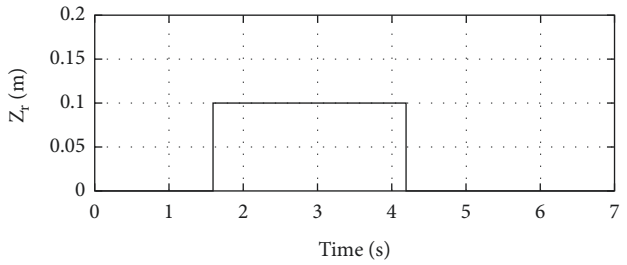


Figure 11: Terrain of the road 2.

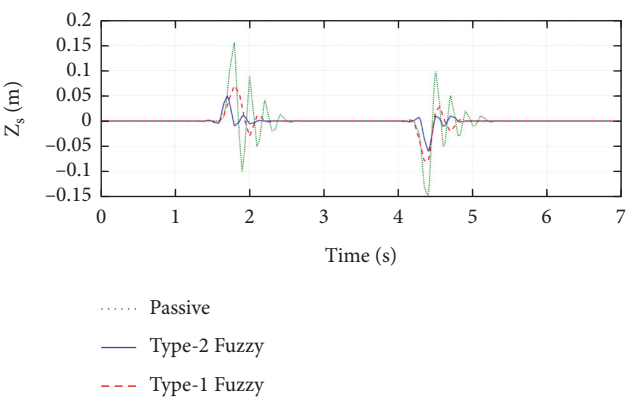


Figure 12: Body displacement (step).

stability. The performance results of the control systems for the acceleration of the body are shown in Figure 9.

The control signals for both active controllers (sliding model with type-1 and type-2 fuzzy systems) are shown in Figure 10.

To further explore and challenge the control system, a step roughness is also applied, as shown in Figure 11.

The performance of all three control systems for roughness is shown in Figures 11 and Figure 12.

Figures 13 and 14 show the speed and acceleration of the body for the roughness of Figure 11, respectively.

Finally, Figure 15 shows the control signals from both active systems for stepped unevenness.

Observing the simulation results, we find that an active control system is essential for vehicles. The active controller has been able to prevent the vehicle body from oscillating

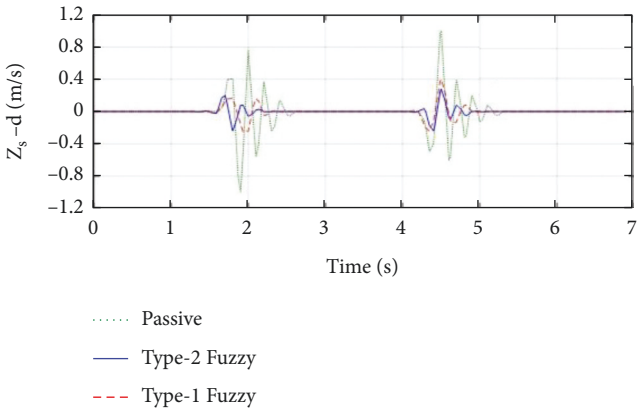


Figure 13: Body velocity (step).

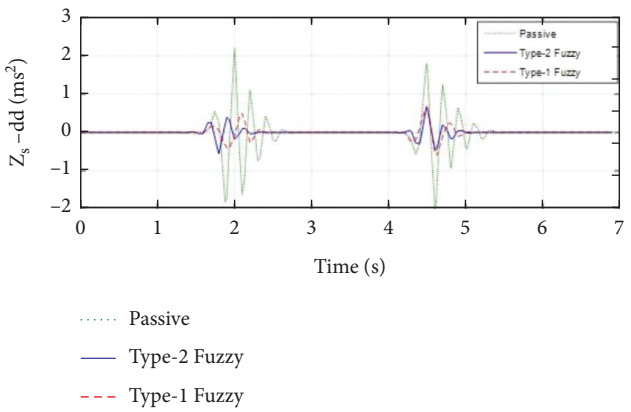


Figure 14: Body acceleration (step).

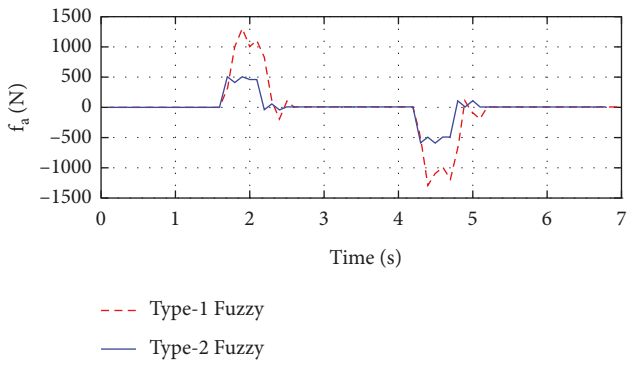


Figure 15: Control signal (step).

well and provide the comfort for the passengers. A 10 cm high step rug, which is one of the most challenging cases in the field of suspension systems, was also applied to our system, and the results show the high capability of the proposed control method.

## 7. Conclusion

The vehicle suspension system has a fundamental and direct effect on the comfort and convenience of the occupants. Therefore, better and more accurate control of this system is necessary and important. In the proposed approach, dynamic sliding mode control is used to improve the performance of the active suspension so that both mechanical and electrical equations of the suspension are considered, this is why the equations used are so complex. Type-1 and type-2 fuzzy systems were used to estimate the sliding mode control parameters. An electric valve is used, and the backlashing valve outlet activates the hydraulic actuator. That is, despite the uncertainties in the system (ground terrains), the only available signal is the inlet current of the valve. Therefore, the smooth flow without chattering of the solenoid valve is calculated in two steps such that the suspension has the desired behavior. The proposed method is without chattering and is also resistant to road uncertainties. New methods such as type-3 fuzzy sliding mode technique can be used to improve this work (as future research). This method has a higher degree of freedom and it has more control parameters. Other uncertainties such as the looseness of the control valve and the nonadjustment of the tire pressure can be considered.

## Data Availability

The numerical data used to support the findings of this study are available from the corresponding author upon request.

## Conflicts of Interest

The authors declare that they have no conflicts of interest.

## References

[1] Z. Li, L. Zheng, Y. Ren, Y. Li, and Z. Xiong, "Multi-objective optimization of active suspension system in electric vehicle with In-Wheel-Motor against the negative electromechanical coupling effects," *Mechanical Systems and Signal Processing*, vol. 116, pp. 545–565, Feb. 2019.

[2] Q. Meng, C. Qian, and R. Liu, "Dual-rate sampled-data stabilization for active suspension system of electric vehicle," *International Journal of Robust and Nonlinear Control*, vol. 28, no. 5, pp. 1610–1623, 2018.

[3] A. Azizi, "A case study on computer-based analysis of the stochastic stability of mechanical structures driven by white and colored noise: utilizing artificial intelligence techniques to design an effective active suspension system," *Complexity*, vol. 2020, Article ID 7179801, 8 pages, 2020.

[4] E. Risaliti, T. Tamarozzi, M. Vermaut, B. Cornelis, and W. Desmet, "Multibody model based estimation of multiple loads and strain field on a vehicle suspension system," *Mechanical Systems and Signal Processing*, vol. 123, pp. 1–25, 2019.

[5] H. Pan and W. Sun, "Nonlinear output feedback finite-time control for vehicle active suspension systems," *IEEE Transactions on Industrial Informatics*, vol. 15, no. 4, pp. 2073–2082, 2019.

[6] G. Long, F. Ding, N. Zhang, J. Zhang, and A. Qina, "Regenerative active suspension system with residual energy for in-wheel motor driven electric vehicle," *Applied Energy*, vol. 260, 2020.

[7] T. A. Nguyen, "Improving the comfort of the vehicle based on using the active suspension system controlled by the double-

integrated controller," *Shock and Vibration*, vol. 2021, Article ID 1426003, 11 pages, 2021.

[8] J. Tavoosi, "Sliding mode control of a class of nonlinear systems based on recurrent type-2 fuzzy RBFN," *International Journal of Mechatronics and Automation*, vol. 7, no. 2, pp. 230–240, 2020.

[9] H. Mobki, A. Majidzadeh Sabegh, A. Azizi, and H. M. Ouakad, "On the implementation of adaptive sliding mode robust controller in the stabilization of electrically actuated micro-tunable capacitor"," *Microsystem Technologies*, vol. 26, no. 12, pp. 3903–3916, 2020.

[10] A. Azizi and H. Mobki, "Applied mechatronics: designing a sliding mode controller for active suspension system," *Complexity*, vol. 2021, Article ID 6626842, 23 pages, 2021.

[11] H. Pang, X. Liu, Y. Shang, and R. Yao, "A hybrid fault-tolerant control for nonlinear active suspension systems subjected to actuator faults and road disturbances," *Complexity*, vol. 2020, Article ID 1874212, 14 pages, 2020.

[12] F. Mohammadi, B. Mohammadi-ivatloo, G. B. Gharehpetian et al., "Robust control strategies for microgrids: a review," *IEEE Systems Journal*, 2021.

[13] A. Azizi, "A case study on designing a sliding mode controller to stabilize the stochastic effect of noise on mechanical structures: residential buildings equipped with ATMD," *Complexity*, vol. 2020, Article ID 9321928, 17 pages, 2020.

[14] S. M. Abtahi, "Suppression of chaotic vibrations in suspension system of vehicle dynamics using chattering-free optimal sliding mode control," *Journal of the Brazilian Society of Mechanical Sciences and Engineering*, vol. 41, no. 5, pp. 1–10, 2019.

[15] Y. Shahid and M. Wei, "Comparative analysis of different model-based controllers using active vehicle suspension system," *Algorithms*, vol. 13, no. 1, 2019.

[16] A. Karami-mollaee, H. Tirandaz, and O. Barambones, "On dynamic sliding mode control of nonlinear fractional-order systems using sliding observer," *Nonlinear Dynamics*, vol. 92, no. 3, pp. 1379–1393, 2018.

[17] H. Nemati, M. Bando, and S. Hokamoto, "Chattering attenuation sliding mode approach for nonlinear systems," *Asian Journal of Control*, vol. 19, no. 4, pp. 1519–1531, 2017.

[18] H. Pang, J. Yang, J. Liang, and Z. Xu, "On enhanced fuzzy sliding-mode controller and its chattering suppression for vehicle semi-active suspension system," *SAE Technical Paper*, vol. 2018, 2018.

[19] A. Abid, I. Sami, H. Ali, M. M. Zaid, H. Ahmad, and N. Ahmad, "Model predictive torque control of three phase induction motor with a robust outer loop controller," in *Proceedings of the 2021 International Conference on Robotics and Automation in Industry (ICRAI)*, pp. 1–5, IEEE, Rawalpindi, Pakistan, October 2021.

[20] H. O. Ozer, Y. Hacioglu, and N. Yagiz, "High order sliding mode control with estimation for vehicle active suspensions," *Transactions of the Institute of Measurement and Control*, vol. 40, no. 5, 2017.

[21] S. Ding, K. Mei, and S. Li, "A new second-order sliding mode and its application to nonlinear constrained systems," *IEEE Transactions on Automatic Control*, vol. 64, no. 6, pp. 2545–2552, 2019.

[22] S. Ding, J. H. Park, and C. C. Chen, "Second-order sliding mode controller design with output constraint," *Automatica*, vol. 112, 2020.

[23] S. Tayebi-haghighi, F. Piltan, and J. M. Kim, "Robust composite high-order super-twisting sliding mode control of robot manipulators," *Robotics*, vol. 7, no. 1, 2018.

[24] Y. N. Golouje and S. M. Abtahi, "Chaotic dynamics of the vertical model in vehicles and chaos control of active suspension system via the fuzzy fast terminal sliding mode control," *Journal of Mechanical Science and Technology*, vol. 35, pp. 31–43, 2021.

[25] H. Yang, Q. Liu, Y. Zhang, and F. Yu, "An adaptive sliding mode fault-tolerant control for semi-active suspensions with magnetorheological dampers based on T-S fuzzy vehicle models," *Journal of Vibration and Control*, 2021.

[26] J. Tavoosi, M. Shirkhani, A. Abdali et al., "A new general type-2 fuzzy predictive scheme for PID tuning," *Applied Sciences*, vol. 11, no. 21, 2021.

[27] M.-W. Tian, A. Mohammadzadeh, J. Tavoosi et al., "A deep-learned type-3 fuzzy system and its application in modeling problems," *Acta Polytechnica Hungarica*, vol. 19, no. 2, 2022.

[28] K. Zare, M. M. Mardani, and N. Vafamand, "Fuzzy-logic-based adaptive proportional-integral sliding mode control for active suspension vehicle systems: kalman filtering approach," *Information Technology and Control*, vol. 48, no. 4, 2019.

[29] A. Muhammed and A. Gavrilov, "Managing the handling–comfort contradiction of a quarter-car system using Kalman filter," *Transactions of the Institute of Measurement and Control*, vol. 43, no. 10, 2021.

[30] V. D. Phan, C. P. Vo, H. V. Dao, and K. K. Ahn, "Actuator fault-tolerant control for an electro-hydraulic actuator using time delay estimation and feedback linearization," *IEEE Access*, vol. 9, pp. 107111–107123, 2021.

[31] J. Tavoosi, A. A. Suratgar, and M. B. Menhaj, "Nonlinear system identification based on a self-organizing type-2 fuzzy RBFN," *Engineering Applications of Artificial Intelligence*, vol. 54, pp. 26–38, 2016.

[32] J. Tavoosi and A. Mohammadzadeh, "A new recurrent radial basis function network-based model predictive control for a power plant boiler temperature control," *International Journal of Engineering*, vol. 34, no. 3, 2021.